Available online at www.sciencedirect.com
ScienceDirect
Ceramics International 35 (2009) 1799–1806
CERAMICS INTERNATIONAL
www.elsevier.com/locate/ceramint

Influence of process parameters on the formation of Silicalite-1 zeolite particles

A. Das, N. Das, M.K. Naskar, D. Kundu, M. Chatterjee *, H.S. Maiti

Sol-Gel Division, Central Glass & Ceramic Research Institute (Council of Scientific & Industrial Research, CSIR), Kolkata 700 032, India

Received 9 July 2008; received in revised form 7 August 2008; accepted 2 October 2008
Available online 21 October 2008

Abstract

Silicalite-1 particles with minimum twinning have been synthesized inside the polar core of non-ionic surfactant/co-surfactant-stabilized water-in-oil (w/o) type emulsions at 150° ± 1 °C within a short reaction time of 5 h. The non-ionic surfactants of varying hydrophilic–lipophilic balance (HLB) values, i.e. sorbitan monooleate (Span 80, HLB: 4.3), sorbitan monolaurate (Span 20, HLB: 8.6), polyoxyethylene (4) lauryl ether (Brij 30, HLB: 9.7) and polyoxyethylene sorbitan monooleate (Tween 80, HLB: 15), the cationic surfactant, i.e. cetyl trimethyl ammonium bromide (CTAB), surfactant concentration, co-surfactant, synthesis temperature and time have been found to play significant role in controlling size and characteristics of Silicalite-1. It has been observed that the crystallinity and size of Silicalite-1 can be tailored by adjusting the interactions between the polar surfactant head groups at the w/o interface and the growing crystallographic surfaces (or silicate/TPA ions) in the aqueous medium of the emulsion.

Keywords: A. Powders: chemical preparation; B. Electron microscopy; B. X-ray methods; D. Silicate

1. Introduction

Zeolites are three-dimensional silicate and aluminosilicate microporous crystalline solids with well-defined structures and pore dimensions from 0.3 to 1 nm [1,2]. Due to varying pore sizes, zeolites can interact very selectively with adsorbed molecules depending on their size, shape and chemical characteristics. The sub nanometre-sized pores in zeolites, makes them useful for molecular sieving membranes, adsorption and catalysis [3–7]. Silicalite-1, the all-silica analogue to the aluminosilicate zeolite ZSM-5, is a porous silica crystal having two interconnected channel systems with pore diameters of 5.2 × 5.7 Å. Due to low dielectric constant, the Silicalite-1 finds important applications for microelectronics [8,9]. It has been observed that particle size and morphology strongly influence the catalytic and separation behaviour of the zeolites [7,10–12].

Synthesis of Silicalite-1 commonly occurs by hydrothermal crystallization in presence of organic structure directing agents. Different silica precursors and structure directing agents generate Silicalite-1 with varying particle size and morphology [13,14]. In addition to the hydrothermal technique, the reverse emulsion method is well accepted for the synthesis of Silicalite-1, as the technique has been proved to be advantageous for the synthesis of particles with controlled growth, small size, better purity, etc. [15–18]. In the emulsion system, in addition to the surfactant, a co-surfactant, typically a straight-chained alcohol such as butanol, pentanol, etc. is often used to aid in lowering the interfacial tension followed by the control of particle size and morphology [11,19]. In our previous study, we have shown the effect of non-ionic surfactants in the Span and Tween series in tailoring the size of oxide and sulphide particles [16,20]. In the present study, we have examined the role of these surfactants in synthesizing Silicalite-1 particles and their characteristics which is not yet well studied. The main reason for considering these non-ionic surfactants is that the absence of any additional ions (cations or anions) helps to avoid ion effects, if any, on the nucleation and growth of the zeolites. Keeping the above points in view, in the present investigation we report (i) an w/o emulsion technique in presence of non-ionic surfactants, i.e. Span 80, Span 20, Brij 30 and Tween 80 with hydrophilic–lipophilic balance (HLB) values of 4.3, 8.6,

* Corresponding author. Tel.: +91 33 24838086; fax: +91 33 24730957.
E-mail address: minati@cgcri.res.in (M. Chatterjee).

0272-8842/$34.00
doi:10.1016/j.ceramint.2008.10.011

9.7 and 15 respectively for the synthesis of Silicalite-1 particles and (ii) the influence of different synthesis parameters like HLB values of non-ionic surfactants and their concentration, presence and absence of co-surfactant, temperature of crystallization and effect of time on the formation of Silicalite-1 crystals in the confined space of the emulsion system. The effect of cationic surfactant, i.e. cetyltrimethylammonium bromide (CTAB) on the crystallization of Silicalite-1 particles in the present w/o type emulsion has also been discussed and the characteristics of the particles are compared with those obtained from the non-ionic surfactants.

2. Experimental procedure

2.1. Synthesis of Silicalite-1 particles

In the present investigation, w/o type emulsions were used for the synthesis of Silicalite-1 zeolite particles. For such synthesis, tetraethylorthosilicate (TEOS ≥98%, Fluka, Switzerland), tetrapropylammonium hydroxide (TPAOH, 1.0 M solution in water, Sigma–Aldrich, U.S.A.), ethanol (dehydrated alcohol, Bengal Chemicals and Pharmaceuticals Ltd., India) and deionised water were used as the starting materials. Required amount of TEOS was taken in a tightly covered polypropylene beaker. Ethanol and water were slowly added under agitation to TEOS. Appropriate quantity of TPAOH was finally added to the above TEOS solution under vigorous stirring, leading to the formation of a clear solution. The molar ratio of the synthesis solution was $3TPAOH:10SiO_2:1500-H_2O:40C_2H_5OH$. This solution was used as the water phase (w) of w/o type emulsions. An organic solvent, i.e. *n*-heptane (G.R., Merck, India) acted as the oil phase (o). A support solvent was prepared by mixing 1 vol% of the non-ionic surfactant, e.g. Span 80 (Fluka Chemie AG, Switzerland) in *n*-heptane. For the preparation of the w/o type emulsions, the water phase was dispersed as droplets in the support solvent under a constant mechanical agitation of 500 rpm and kept under such condition for 15 min for equilibration. The volume ratio of the water phase: support solvent was kept constant at 1:4 in all the experiments.

The synthesis reaction was performed in a Teflon container fitted inside a stainless steel autoclave. The entire emulsion was then taken in the Teflon container of the autoclave. The autoclave was finally sealed and placed in an air oven preheated at 150 ± 1 °C. For controlled growth of the particles, the emulsion was aged at 150 ± 1 °C for 5 h and then removed from air oven. The entire emulsion was cooled down to the ambient temperature and added to a known volume of methanol (G.R., Merck, India) (volume ratio of emulsion: methanol = 1:5). Immediate flocculation of particles occurred which were collected by centrifugation at 9000 rpm. To remove last traces of adhered impurities, the particles were washed thrice with methanol, each time collecting the particles centrifugally as described above followed by the dispersion in the washing solvents. The washed particles were dried at 80 °C. Following the same procedure, Silicalite-1 particles were prepared under different experimental conditions as presented in Table 1. In addition to Span 80, other non-ionic surfactants like Span 20 (Fluka Chemie AG, Switzerland), Brij 30 (Sigma–Aldrich, U.S.A.), Tween 80 (Fluka Chemie AG, Switzerland) and the cationic surfactant, CTAB (BDH Chemical Ltd., England, 98%), as presented in Table 1, were also used for the stabilization of emulsions. The *n*-butanol (Rankem India, 99.5%) acted as the co-surfactant in some of the experiments. Fig. 1 depicts a schematic for the formation of emulsion-derived Silicalite-1 zeolite particles. In this figure, Step I indicates the formation of surfactant and co-surfactant stabilized aqueous (zeolitic) microdroplets inside the polar core of the w/o emulsion, Step II presents formation of Silicalite-1 crystals inside the confined aqueous microdroplets during heating and finally Step III indicates free-standing Silicalite-1 crystals after breaking the emulsion with methanol.

2.2. Characterization of the zeolite particles

The zeolite particles were subjected to X-ray powder diffraction (XRD; Model: Philips, 1730, U.S.A.) with Ni-filtered Cu Kα radiation to identify the phases crystallized under different experimental conditions. The relative crystallinity of Silicalite-1 synthesized in presence of Span 80, Span

Table 1
Experimental conditions for the synthesis of Silicalite-1 crystals from w/o emulsion and the characteristics of the particles obtained there from.

Surfactant	Co-surfactant	Surfactant concentration	Surfactant: co-surfactant (by wt.)	Temperature (°C)	Time (h)	Average particle size (d_{50}) (μm)	Surface area (m^2/g)	Ignition loss (wt.%)
Span 80 (HLB: 4.3)	–	1 vol%	–	150	5	2.3	193	25.2
Span 20 (HLB: 8.6)	–	1 vol%	–	150	5	2.8	82.3	16.0
	n-butanol	1 vol%	2:1	150	5	2.2	85.5	16.2
	n-butanol	3 vol%	2:1	150	5	3.0	92.9	32.8
	n-butanol	1 vol%	2:1	150	3	2.0	90.1	12.9
	n-butanol	1 vol%	2:1	130	5	2.1	88.3	13.8
	n-butanol	1 vol%	1:1	150	5	2.7	85.4	14.5
Brij 30 (HLB: 9.7)	–	1 vol%	–	150	5	3.0	80.3	15.9
Tween 80 (HLB: 15)	–	1 vol%	–	150	5	1.8	141.3	33.8
	n-butanol	1 vol%	2:1	150	5	2.7	132.7	32.1
CTAB	–	1 wt%	–	150	5	15.8	382.4	34.8
	n-butanol	1 wt%	2:1	150	5	16.7	390.1	35.5

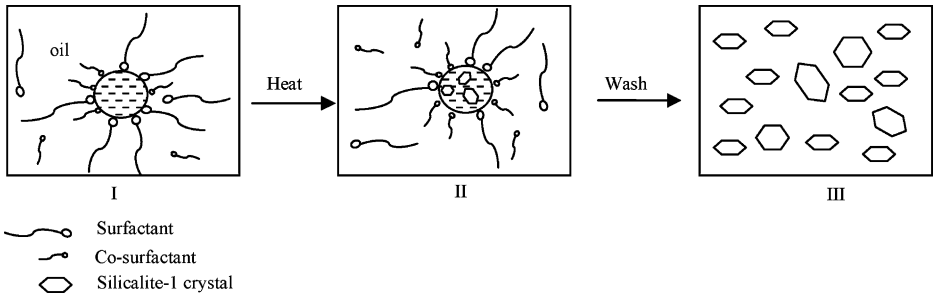

Fig. 1. A schematic for the synthesis of Silicalite-1 particles from the non-ionic surfactant-/co-surfactant-stabilized emulsion.

20, Brij 30, and Tween 80 (without co-surfactant in each case) was analyzed comparing the intensities of five diffraction peaks in the 2θ range of 22–25° [21]. The sample with the highest integrated intensities of diffraction peaks was considered as the 100% crystalline, i.e. as the reference. In the present investigation, the Brij 30-derived Silicalite-1 was considered as the reference, as it exhibited the maximum integrated intensity of diffraction peaks in the 2θ range of 22–25°. The morphology of the particles was examined by scanning electron microscopy (SEM; Model: LEO S430i, U.K.) and transmission electron microscopy (TEM; Model: JEOL 2110, Japan). The average particle size (d_{50}) of the samples, dried at 100 °C for 1 h, was determined by dynamic light scattering method using the particle size analyzer (Model: Mastersizer 2000, Malvern Instruments Ltd., Malvern, U.K.). The specific surface area of the particles, calcined at 500 °C with a dwell time of 1 h, was measured using the BET surface area analyzer (Model: Autosorb 1, Quantachrome Corporation, U.S.A.). Ignition loss due to loss of adsorbed organics and other volatiles was determined by heating the samples at 500 °C with a dwell time of 1 h in a programmable electric furnace in air atmosphere. The results are summarized in Table 1.

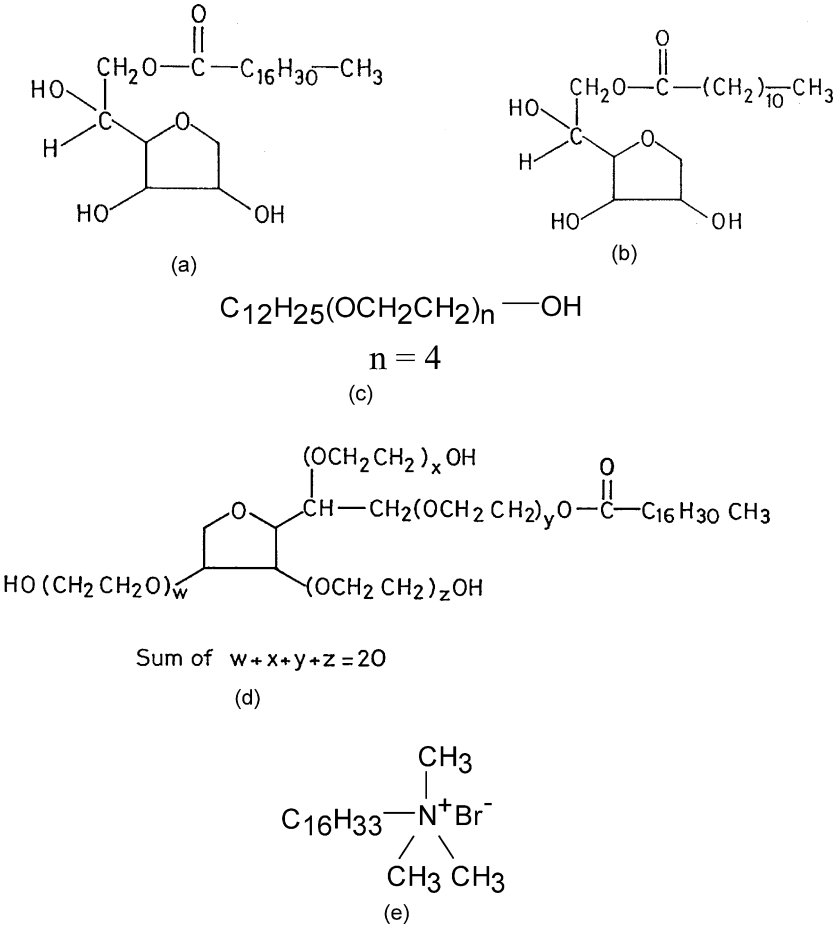

Fig. 2. Molecular structures of amphiphilic surfactants: (a) Span 80 (HLB: 4.3); (b) Span 20 (HLB: 8.6); (c) Brij 30 (HLB: 9.7); (d) Tween 80 (HLB: 15) and (e) CTAB.

3. Results and discussion

3.1. Stabilization of the aqueous zeolitic microdroplets

In a system composed of two immiscible liquids, i.e. for the w/o type emulsions in the present investigation, dispersion of the water phase (zeolitic solution) in the oil phase (*n*-heptane) as small droplets under agitation causes an increase in the surface area of the dispersed phase. Thermodynamically, the increase in surface area 'ΔA' of the dispersed phase associated with a free energy change (ΔG) can be represented as [22]

$$\Delta G = \gamma \Delta A \quad (1)$$

where γ is the interfacial tension. The equation indicates that a low interfacial tension favours droplet disruption. In fact, this is accomplished by the addition of a system compatible amphiphilic surface active agent or surfactant which gets adsorbed on the dispersed aqueous droplets and prevents their coalescence by the steric hindrance. The droplet size is tailored with the type and amount of the surfactant, co-surfactant, synthesis time and temperature, etc. [16,23]. Thus, the surfactant added to the system (i) lowers the interfacial tension between two immiscible liquids, favouring droplet disruption and (ii) prevents re-coalescence of the aqueous droplets by adsorbing on their surfaces, thus producing a stable emulsion. In the present investigation, non-ionic surfactants like Span 80, Span 20, Brij 30 and Tween 80 of HLB values of 4.3, 8.6, 9.7 and 15, respectively and the cationic surfactant, CTAB, have been used for the stabilization of emulsions. Fig. 2 presents the molecular structures of the amphiphilic surfactants used in the present study.

The non-ionic surfactants used for the stabilization of the aqueous droplets are characterized by their HLB values. A high HLB value of the surfactant indicates strongly hydrophilic character, while a low value is an indication of a strong hydrophobic nature. Considering these points, non-ionic surfactants, e.g. Span 80, Span 20, Brij 30 and Tween 80 of HLB values of 4.3, 8.6, 9.7 and 15 respectively have been selected in the present study for understanding their role in particle formation. The cationic surfactant, CTAB, has been used to compare the results obtained with those of the non-ionic surfactants. The sorbitan group in Fig. 2(a) and (b), the polyoxyethylene group in Fig. 2(c) and the polyoxyethylene sorbitan group in Fig. 2(d) act as the hydrophilic ''polar head'' while the oleic acid group in Fig. 2(a) and (d), lauric acid in Fig. 2(b) and the lauryl group in Fig. 2(c) act as the hydrophobic ''non-polar tail''. In CTAB (Fig. 2e), the ammonium ion and the

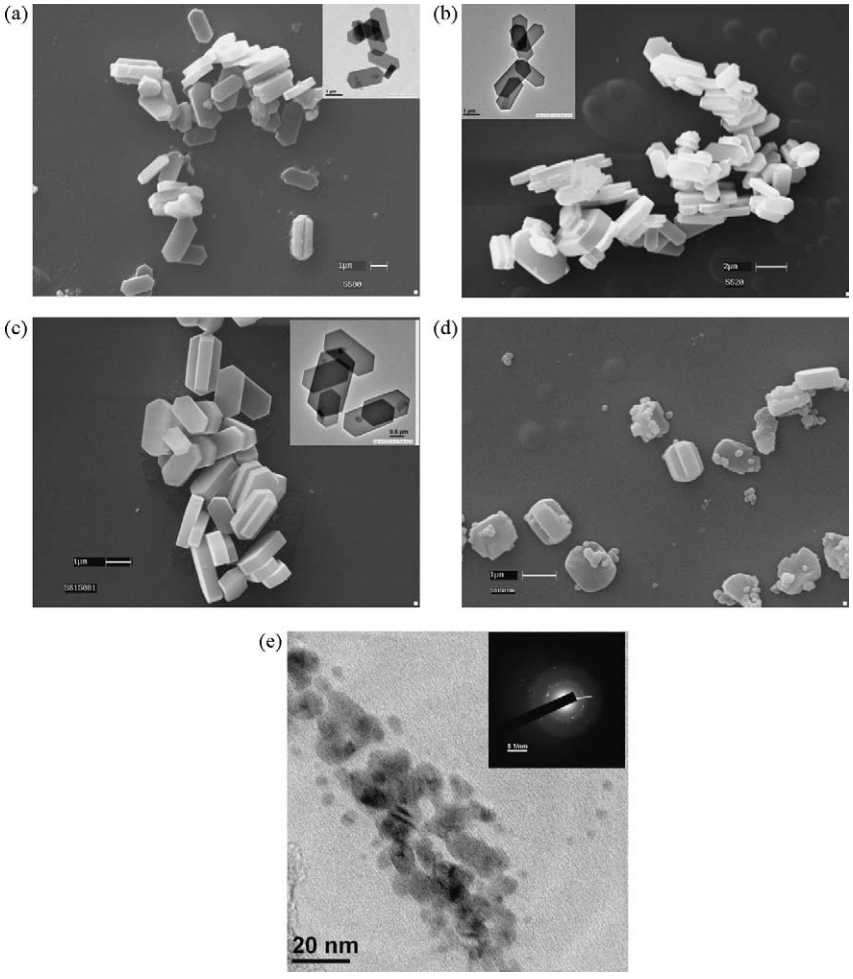

Fig. 3. SEM and TEM images of the emulsion-derived Silicalite-1 particles crystallized at 150 ± 1 °C/5 h in presence of different surfactants (in the absence of co-surfactant): (a) Span 80 (HLB: 4.3); (b) Span 20 (HLB: 8.6); (c) Brij 30 (HLB: 9.7); (d) Tween 80 (HLB: 15) and (e) CTAB.

cetyltrimethyl parts act as the ''polar head'' and the ''non-polar tail'', respectively.

3.2. Formation of Silicalite-1 particles

The formation conditions of Silicalite-1 crystals, employed in this work, are summarized in Table 1. The variation emphasized mainly on the nature and concentration of the surfactants, effect of co-surfactant and also on the synthesis temperature and time. The influence of process parameters on the crystallization behaviour of Silicalite-1 zeolite particles has been studied by SEM, TEM and XRD. The following sections present the observations.

3.2.1. Role of surfactants

Fig. 3 presents the SEM and TEM images of Silicalite-1 synthesized inside the polar core of w/o emulsions stabilized in presence of non-ionic and cationic surfactants (in the absence of co-surfactant). SEM images of non-ionic surfactant derived Silicalite-1 crystals in Fig. 3(a)–(d) indicate that the particles are of coffin-shaped morphology. In addition, all the coffin-shaped crystals in Fig. 3(b) and (c) have smooth surfaces and contain less twinning. This is supported from TEM images shown at the inset of the respective SEM micrographs of the samples. The crystal surfaces in Fig. 3(a) are not as smooth as observed in Fig. 3(b) and (c). In Fig. 3(d), the small-sized (1 μm × 0.5 μm × 0.3 μm approx.), coffin-shaped/rounded crystals are associated with some irregular-shaped particles. The situation is, however, totally different in the case of the ionic surfactant, the CTAB-derived particles (Fig. 3e). In this case, the TEM image shows that the material exists as agglomerates of spherical particles. XRD patterns (Fig. 4) of all the samples in Fig. 3 have been recorded for supporting information.

Fig. 4(a)–(d) illustrates the XRD patterns of samples obtained in presence of non-ionic surfactants like Span 80 (HLB: 4.3), Span 20 (HLB: 8.6), Brij 30 (HLB: 9.7), Tween 80 (HLB: 15), respectively and Fig. 4(e) the ionic surfactant, CTAB-stabilized emulsion in the present investigation. The XRD results indicate that all the samples in Fig. 4(a)–(d) crystallized to Silicalite-1 as the only phase; no other impurity phases are found to be present. Depending on the surfactant identity, the crystallinity of the sample was, however, found to be different and estimated as 77%, 84%, 100% and 50% for Span 80, Span 20, Brij 30 and Tween 80-derived Silicalite-1 zeolite, respectively. The above data indicate that the crystallinity of the particles increases with the increase in the HLB value of up to 9.7 of Brij 30; further increase in HLB value to 15, however, the intensity of the XRD peaks becomes quite small, i.e. the small particles of approximate size 1 μm × 0.5 μm × 0.3 μm (as observed under SEM) exhibit less crystallinity. This is in contrast to the samples synthesized in the polar core of the CTAB-stabilized emulsions as shown in Fig. 4(e). It is observed from Fig. 4(e) that the amorphous silica is identified under the present set of experimental condition. Therefore, the spherical agglomerates in TEM image correspond to amorphous silica.

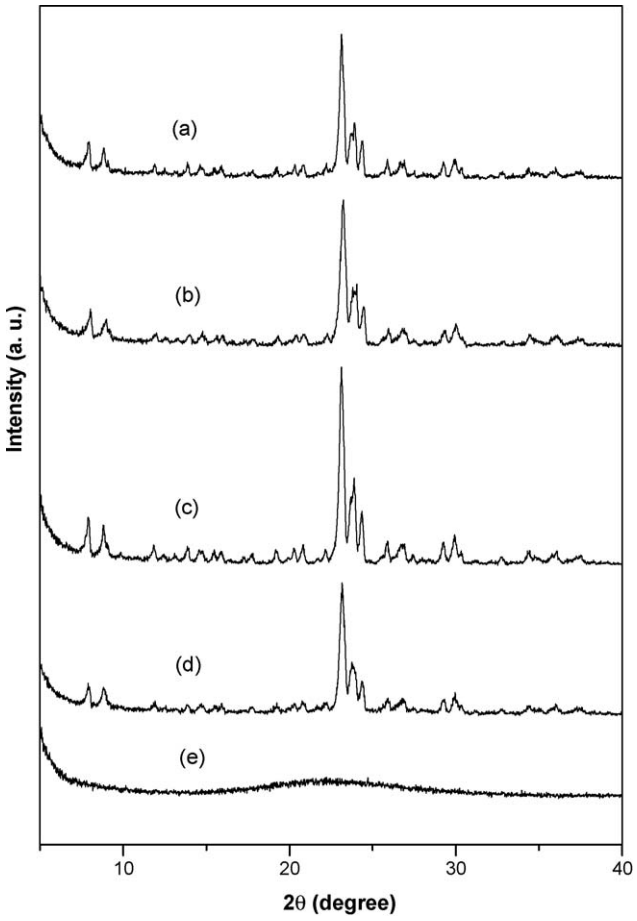

Fig. 4. XRD patterns of the emulsion-derived Silicalite-1 particles crystallized at 150 ± 1 °C/5 h in presence of different surfactants (in the absence of co-surfactant): (a) Span 80 (HLB: 4.3); (b) Span 20 (HLB: 8.6); (c) Brij 30 (HLB: 9.7); (d) Tween 80 (HLB: 15) and (e) CTAB.

Considering the molecular structure (Fig. 2) and HLB values of the non-ionic surfactants, i.e. Span 80 (HLB: 4.3), Span 20 (HLB: 8.6) and Brij 30 (HLB: 9.7), it is to be noted that the increase in the HLB value causes an increase in hydrophilicity in the surfactants, leading to increase in interaction between the polar surfactant head groups and water dipoles. This brings about a gradual decrease in interfacial tension at the w/o interface, followed by higher water solubilization. This surfactant–water interaction, on the other hand, causes a gradual decrease in interaction between the surfactant–silicate/TPA species [19] and thus facilitating the TPA–silicate electrostatic forces and nucleation of Silicalite-1 crystals. With further increase in HLB value to 15 in Tween 80 (resulting in the higher hydrophilicity due to the presence of 20 numbers of polyoxyethylene groups in the sorbitan part of the surfactant), in addition to the above-mentioned surfactant–water interaction, surfactant–silicate/TPA ion interaction takes place also which inhibits crystallization of Silicalite-1 under identified experimental conditions. Due to such interactions, decrease in crystallinity and size of the Silicalite-1 particles is observed.

In the case of CTAB-stabilized emulsions, the strong electrostatic forces between the anionic silicate species and the

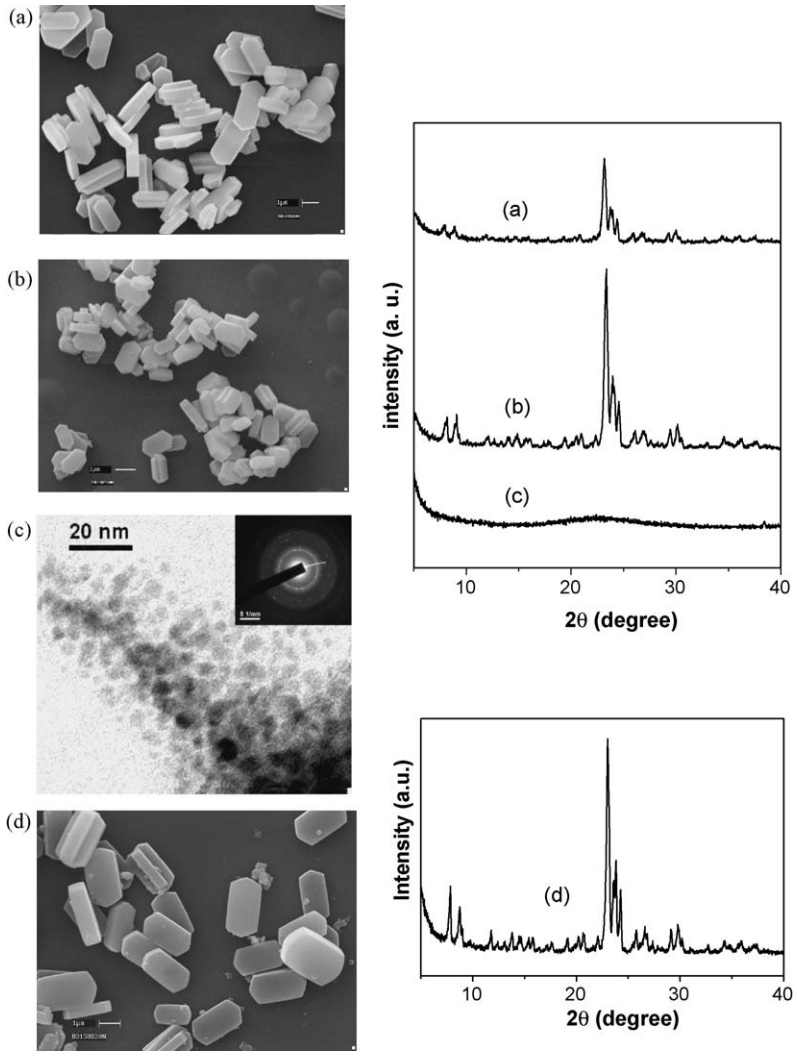

Fig. 5. Micrographs (SEM and TEM images) and XRD patterns of the emulsion-derived Silicalite-1 particles with different composition of surfactant and *n*-butanol (weight ratio) crystallized at 150 ± 1 °C/5 h. Surfactant: *n*-butanol = 2:1 (a) Span 20 (HLB: 8.6)/*n*-butanol (SEM image); (b) Tween 80 (HLB: 15)/*n*-butanol (SEM image) and (c) CTAB/*n*-butanol (TEM image) and surfactant:*n*-butanol = 1:1 (d) Span 20 (HLB: 8.6)/*n*-butanol (SEM image).

cationic head groups of the surfactant are responsible for hindering the nucleation of Silicalite-1 crystals and formation of aggregates of amorphous silica particles. Therefore, SEM/TEM results in Fig. 3 are consistent with those of XRD as presented in Fig. 4.

3.2.2. Role of co-surfactant

The characteristics of Silicalite-1 crystals obtained in this work were found to depend also on the presence of *n*-butanol, the co-surfactant, along with the surfactants [23]. The function of the co-surfactant is to reduce the w/o interfacial tension by

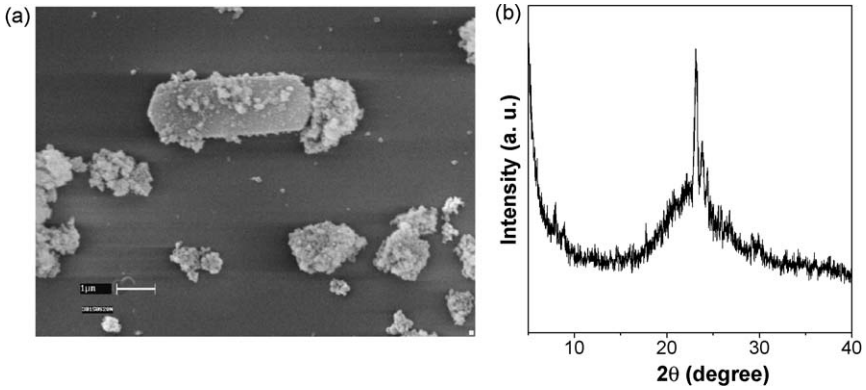

Fig. 6. SEM image (a) and XRD (b) pattern of the emulsion-derived Silicalite-1 particles crystallized at 150 ± 1 °C/5 h in presence of higher quantity of Span 20 (3 vol%) and co-surfactant, *n*-butanol.

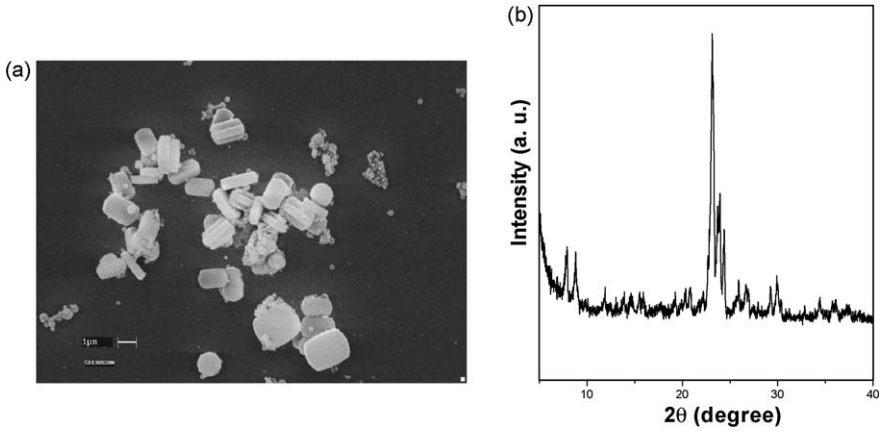

Fig. 7. SEM image (a) and XRD pattern (b) of the emulsion-derived Silicalite-1 particles crystallized at lower temperature, i.e. 130 ± 1 °C/5 h in presence of the surfactant Span 20 and co-surfactant *n*-butanol.

adsorbing at the interface and minimize the repulsion between the hydrophilic head groups (Fig. 1), resulting in higher water solubilization and decrease in water droplet size. To examine the effect of co-surfactant on the growth of Silicalite-1 crystals, *n*-butanol was added to the Span 20, Tween 80 and CTAB-stabilized emulsions initially in the 2:1 weight ratio of the surfactant: co-surfactant. Fig. 5 exhibits the SEM, TEM and XRD results. We have already observed in Fig. 3(b) that in the absence of *n*-butanol, the Span 20 stabilized synthesis reaction gives rise to Silicalite-1 crystals of larger dimensions (3.4 μm × 1.5 μm × 0.6 μm approx.) with wide size distribution. However, in presence of *n*-butanol, the particles in Fig. 5(a) become smaller (2.5 μm × 1 μm × 0.4 μm approx.) and more uniform in size. XRD spectra (Fig. 5(a)) of the same clearly support the results. In the case of Tween 80-stabilized emulsion, the presence of *n*-butanol in 2:1 weight ratio with the surfactant at the w/o interface screen the attractive force between the surfactant head groups and silicate/TPA species and facilitate the growth of Silicalite-1 crystals as evidenced by SEM and XRD (Fig. 5(b)) studies. The size of the particles is quite uniform (1.5 μm × 0.9 μm × 0.4 μm approx.) as observed under SEM. In the case of CTAB-stabilized emulsion system, presence of *n*-butanol in 2:1 weight ratio with the surfactant, both TEM and XRD (Fig. 5(c)) did not indicate any sign of crystallization of Silicalite-1. The TEM image exhibits the formation of very small, i.e. 1–5 nm in size and well dispersed amorphous silica particles. However, increase in butanol content (surfactant:*n*-butanol weight ratio to 1:1) at the interface of the emulsion (Fig. 1), causes an increase in crystal size, as presented in Fig. 5(d). XRD analysis (Fig. 5(d)) also supports the result. Increase in butanol content should effectively screen the interaction between the surfactant–silicate/TPA species, thereby increasing the crystal size.

Therefore, from the above results it is inferred that not only surfactant molecules but the co-surfactant also plays an important role in tailoring the size, morphology and crystallinity of the particles by controlling the interactions between the polar head groups and the silicate/TPA species or crystallographic faces of the growing crystals in emulsion systems.

3.2.3. Role of surfactant content

Increase in surfactant content also affects the growth of Silicalite-1 crystals as manifested by the SEM and XRD results in Fig. 6(a) and (b), respectively. The SEM image supported by the XRD result shows that the decrease in the size of Silicalite-1 is observed as the content of the surfactant Span 20 is increased from 1 vol% to 3 vol% with respect to *n*-heptane. XRD results also indicate the presence of considerable amount of amorphous

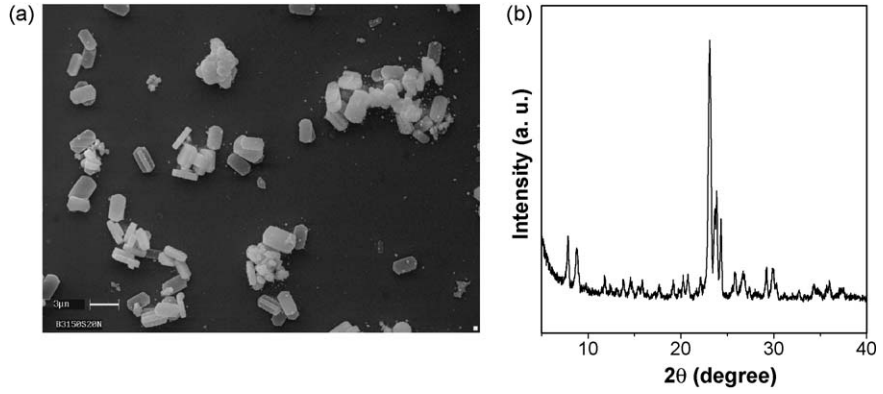

Fig. 8. SEM image (a) and XRD pattern (b) of the emulsion-derived Silicalite-1 particles crystallized at 150 ± 1 °C and less reaction time of 3 h in presence of the surfactant Span 20 and co-surfactant *n*-butanol.

phase. Appearance of irregular-shaped materials along with the Silicalite-1 crystals in SEM supports the XRD observations. Increase in attractive forces between the increased amount of polar surfactant head groups and the silicate/TPA ions significantly affect the growth of Silicalite-1 crystals.

3.2.4. Role of synthesis temperature and time

The effect of synthesis temperature (Fig. 7(a) and (b)) and time (Fig. 8(a) and (b)) on the formation of Silicalite-1 crystals inside the polar core of the Span 20-stabilized emulsion was also examined by SEM and XRD studies. Decrease in synthesis temperature from 150 to 130 °C or decrease in reaction time from 5 to 3 h leads to incomplete crystallization of Silicalite-1 particles as evidenced by the presence of irregular-shaped materials along with the coffin-shaped crystals in SEM images. Therefore, in the present investigation, synthesis temperature of 150 °C and the synthesis time of 5 h have been proved to be the optimum.

4. Conclusions

We have reported an effective method for in situ synthesis of coffin-shaped Silicalite-1 zeolite (with minimum twinning) at 150 °C inside the polar core of non-ionic surfactant stabilized w/o type emulsion within a very short reaction time of 5 h. The effect of non-ionic surfactants like Span 80 (HLB: 4.3), Span 20 (HLB: 8.6), Brij 30 (HLB: 9.7) and Tween 80 (HLB: 15) with different structure type and hydrophilicity has been found to have significant effect on the nucleation and growth of Silicalite-1 particles. In addition, the concentration of surfactant, presence of co-surfactant, i.e. *n*-butanol, synthesis temperature and time also influenced the characteristics and growth of zeolite crystals. We have also shown that the crystallinity and size of Silicalite-1 can be tailored by adjusting the interaction between the polar surfactant head groups at the w/o interface and the growing crystallographic surfaces (or silicate/TPA ions) in the aqueous medium of the emulsion. In the case of CTAB-stabilized emulsion, the strong electrostatic forces between the anionic silicate species and the cationic head groups hinder the nucleation of Silicalite-1 crystals under the identical experimental conditions and resulted in the formation of amorphous silica. The present method has been found to be highly useful for synthesizing coffin-shaped particles of controlled size from the non-ionic surfactant stabilized emulsion. Silicalite-1 crystals find applications as seeds for zeolite membrane formation through secondary hydrothermal growth.

Acknowledgements

The authors thank Dr. H.S. Maiti, Director of the Institute, for his kind permission to publish this paper. Thanks are also due to the colleagues of the XRD and SEM sections for rendering help in material characterization. The financial support received from the Council of Scientific and Industrial Research (CSIR), New Delhi, in the Project No. SIP 0023 is also thankfully acknowledged.

References

[1] D.W. Breck, Zeolite Molecular Sieves: Structure Chemistry and Use, Wiley, New York, 1974.
[2] R.M. Barrer, Zeolite and Clay Minerals as Sorbents and Molecular Sieves, Academic Press, London, 1978.
[3] X. Nu, W. Yang, J. Liu, L. Lin, N. Stroh, H. Brunner, Synthesis of NaA zeolite membrane on a ceramic hollow fibre, J. Membr. Sci. 229 (1–2) (2004) 81–85.
[4] J.M. van de Graaf, F. Kapteijn, J.A. Moulign, Methodological and operational aspects of permeation measurements on silicalite-1 membranes, J. Membr. Sci. 144 (1–2) (1998) 87–104.
[5] J.A. Vroon, K. Keizer, M.J. Glide, J. Verweij, A.J. Burggraaf, Transport properties of alkanes through ceramic thin zeolite MFI membranes, J. Membr. Sci. 113 (2) (1996) 293–300.
[6] E.G. Derouane, New aspects of molecular shape selectivity, in: B. Imelik, C. Naccache, Y. Ben Taarit, J.C. Vedrine, H. Praliaud (Eds.), Catalysis by Zeolites, Studies in Surface Science and Catalysis 5, Elsevier Scientific Publishing Company, Amsterdam, 1980, pp. 5–17.
[7] M.M.J. Treacy, B.K. Marcus, M.E. Bisher, J.B. Higgins (Eds.), Proceedings of the 12th International Zeolite Conference, Edited by Materials Research Society, Pennsylvania, U.S.A., 1999.
[8] Z.B. Wang, A. Mitra, H.T. Wang, L.M. Huang, Y.H. Yan, Pure silica zeolite films as low-k dielectrics by spin-on of nanoparticle suspensions, Adv. Mater. 13 (19) (2001) 1463–1466.
[9] Z.B. Wang, H.T. Wang, A. Mitra, L.M. Huang, Y.S. Yan, Pure silica zeolite low-k dielectric thin films, Adv. Mater. 13 (10) (2001) 746–749.
[10] M.E. Davis, Ordered porous materials for emerging applications, Nature 417 (6891) (2002) 813–821.
[11] J.C. Lin, M.J. Yates, Altering the crystal morphology of silicalite-1 through microemulsion-based synthesis, Langmuir 21 (6) (2005) 2117–2120.
[12] Z. Chen, S. Li, Y. Yan, Synthesis of template-free zeolite nanocrystals by reverse microemulsion–microwave method, Chem. Mater. 17 (9) (2005) 2262–2266.
[13] T. Kida, K. Kojima, H. Ohnishi, G. Guan, A. Yoshida, Synthesis of large silicalite-1 single crystals from two different silica sources, Ceram. Int. 30 (5) (2004) 727–732.
[14] P.-P.E.A. de Moor, T.P.M. Beelen, R.A. van Santen, L.W.B. Beck, M.E. Davis, Si-MFI crystallization using a ‘‘dimer’’ and ‘‘trimer’’ of TPA studied with small angle X-ray scattering, J. Phys. Chem. B 104 (32) (2000) 7600–7611.
[15] F.J. Arriagada, K. Osseo-Asare, Synthesis of nanosize silica in Aerosol OT reverse microemulsions, J. Colloid Interf. Sci. 170 (1) (1995) 8–17.
[16] M.K. Naskar, A. Patra, M. Chatterjee, Understanding the role of surfactants on the preparation of ZnS nanocrystals, J. Colloid Interf. Sci. 297 (1) (2006) 271–275.
[17] M. Chatterjee, M.K. Naskar, Synthesis of yttrium–aluminium–garnet hollow microspheres by reverse-emulsion technique, J. Am. Ceram. Soc. 89 (4) (2006) 1443–1446.
[18] M.K. Naskar, M. Chatterjee, Magnesium aluminate ($MgAl_2O_4$) spinel powders from water-based sols, J. Am. Ceram. Soc. 88 (1) (2005) 38–44.
[19] S. Lee, C. Shane Carr, D.F. Shantz, Anioic microemulsion-mediated low temperature synthesis of anisotropic silicalite-1 nanocrystals, Langmuir 21 (25) (2005) 12031–12036.
[20] M. Chatterjee, M.K. Naskar, B. Siladitya, D. Ganguli, Role of organic solvents and surface-active agents in the sol–emulsion–gel synthesis of spherical alumina powders, J. Mater. Res. 15 (1) (2000) 176–185.
[21] H. Liu, G. Lu, H. Hu, Synthesis, characterization and catalytic performance of titanium silicalite-1 prepared in presence of non-ionic surfactants, Mater. Chem. Phys. 100 (1) (2006) 162–167.
[22] E. Dickinson, Emulsion and droplet size control, in: D.J. Wedlock (Ed.), Controlled Particle, Droplet and Bubble Formation, Buttworth-Heinemann, Oxford, 1994, pp. 191–216.
[23] T. Charinpanitkul, A. Chanagul, J. Dutta, U. Rungsardthong, W. Tanthapanichakoon, Effects of cosurfactant on ZnS nanoparticle synthesis in microemulsion, Sci. Technol. Adv. Mater. 6 (3–4) (2005) 266–271.